ACS Catalysis

pubs.acs.org/acscatalysis

Research Article

Energetics of Adsorbed Formate and Formic Acid on Cu(111) by Calorimetry

Griffin Ruehl,[§] S. Elizabeth Harman,[§] Olivia M. Gluth, David H. LaVoy, and Charles T. Campbell*

Cite This: *ACS Catal.* 2022, 12, 10950−10960

Read Online

ACCESS | Metrics & More | Article Recommendations

ABSTRACT: The heats of adsorption of formic acid molecularly adsorbed on clean Cu(111) and dissociatively adsorbed on oxygen-predosed Cu(111) were measured by adsorption calorimetry. The dissociative adsorption of formic acid on oxygen-predosed Cu(111) at 240 K produces adsorbed bidentate formate and gaseous water. For this, the differential heat of adsorption is initially 99 kJ/mol, decreasing to 80.4 kJ/mol by ∼0.20 ML. This is (to our knowledge) the only experimental measurement of the energy of *any* molecular fragment bonded to *any* clean and well-ordered Cu single-crystal surface, making these results important benchmarks for validating the energy accuracy of computational models for a wide range of adsorbates on Cu catalysts. The integral (average) heat of adsorption at 240 K and 0.20 ML is 89.7 kJ/mol. From this, the heat of formation of bidentate formate and its bond enthalpy to Cu(111) were determined to be approximately −465 and 335 kJ/mol, respectively. Corresponding values were estimated for monodentate formate on Cu(111), giving −437 and 307 kJ/mol. Comparing these values to previous calorimetric results on Pt(111) and Ni(111) shows that the bond enthalpies and enthalpies of formation of formate on Cu(111) are similar to those on Ni(111) but ∼75 kJ/mol stronger than on Pt(111). Comparing these to reported DFT calculations shows that DFT systematically underestimated the stability of formate on these metals by ∼50 kJ/mol. The differential heat of molecular adsorption of formic acid on clean Cu(111) at 120 K is initially 81 kJ/mol, dropping to ∼70 kJ/mol by ∼0.50 ML, before decreasing to a multilayer energy of 64.3 kJ/mol. Using this heat of adsorption through bulk-like multilayer coverages, we estimate the adhesion energy for liquid formic acid to Cu(111) to be 0.27 J/m^2.

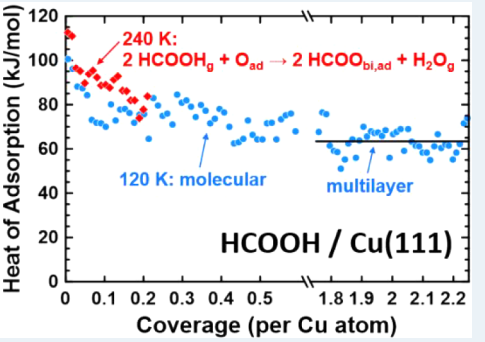

KEYWORDS: *adsorption calorimetry, adsorption energy, adsorbed formate, formic acid dissociation, copper, solvent effects*

1. INTRODUCTION

Understanding the energetics of small molecules and molecular fragments on transition metal surfaces is crucial for advancing fundamental insights into catalysis, developing new catalysts and catalytic processes, and improving the energy accuracy of methods like density functional theory (DFT) used for computational modeling of these systems. Here, we expand upon the previous work of the Campbell group that measured the energetics of irreversible adsorption for molecular fragments on Pt(111) and Ni(111) to now include adsorption on the Cu(111) surface.[1−13] In this paper, we use calorimetry under ultrahigh vacuum conditions to directly measure the heat of molecular adsorption of formic acid onto clean Cu(111), and the heat of dissociative adsorption of formic acid onto oxygen-predosed Cu(111). We compare and contrast these heats on Cu(111) with those measured for the same adsorbates on Pt(111) and Ni(111), and with DFT predictions of these heats on Cu(111).

Formic acid and adsorbed formate are considered important intermediates for many reactions on late transition metal catalysts. This includes well-established industrial reactions such as methanol synthesis, water−gas shift, and steam reforming of methane,[14−17] as well as more emergent applications such as biomass reforming, fuel cell feeds, and a potential hydrogen carrier.[18−22] The surface interactions of organic molecules containing −COO$^-$ or −COOH groups such as peptides, proteins, and amino acid residues are also important for a wide variety of applications ranging from medical implants[23,24] to the controlled synthesis of nanoparticles and nanostructures.[25,26] More recently, formate has emerged as an adsorbed intermediate of interest in thermal and electrocatalytic processes for the reduction of CO_2.[27−29] Thus, reaction pathways for these processes are the subject of intense study.[18,19,21,22,30−32] The results reported here provide

Received: May 29, 2022
Revised: July 30, 2022
Published: August 23, 2022

https://doi.org/10.1021/acscatal.2c02608
ACS Catal. 2022, 12, 10950−10960

important benchmarks to improve the energy accuracy of computational models that seek to elucidate these processes.

Formate is the simplest example of a carboxylate adsorbate and can consequently act as a prototype for understanding the bonding energetics for more complex examples of this class of adsorbates. However, since the dissociative adsorption of formic acid is an irreversible adsorption process, traditional methods for studying the energetics of surface adsorbates, such as temperature-programmed desorption (TPD), cannot be used. To date, the heat of formation of adsorbed formate has only been measured for two surfaces, Pt(111)[6] and Ni(111),[13] both previously reported by this group. This work not only expands these results to the Cu(111) surface but also constitutes (to our knowledge) the only measured heat of formation for *any* molecular fragment on *any* well-defined Cu surface (i.e, any clean and well-ordered single-crystalline Cu surface).

Copper is an important transition metal catalyst for a number of chemical applications where formate and more complex carboxylates are adsorbed intermediates, including water−gas shift, methanol synthesis, partial oxidation of methanol, and the conversion between esters and alcohols.[14−17,33] It has also garnered interest as the most promising monometallic catalyst for CO_2 reduction chemistry, particularly in electrocatalytic applications.[28,34−36] Formate is commonly seen in these reactions as an intermediate in either preferred or competing reaction pathways.[27−29] Additionally, Cu is predicted by DFT to show large differences in adsorbate bond energies in comparison to Ni and Pt. Thus, in combination with previous studies from this group on Pt(111) and Ni(111), these measurements on Cu(111) provide a set of key experimental benchmarks on these three surfaces. As all three of these metals are widely used in industrial catalytic reactions, this suite of benchmarks can expand our fundamental understanding of observed differences in catalytic activity between them. The (111) surface is chosen for all three metals as it is the most thermodynamically stable facet and thus is expected to dominate the surfaces of these metal catalysts, at least when particle size is large. Consequently, the (111) surface has been widely studied as a well-defined model for Cu, Ni, and Pt catalysts.

Here, we use calorimetry under ultrahigh vacuum conditions to directly measure the heat of molecular adsorption of formic acid onto clean Cu(111), and the heat of dissociative adsorption of formic acid onto oxygen-predosed Cu(111). This allows for the extraction of the bond enthalpy and enthalpy of formation of adsorbed bidentate formate on Cu(111), along with estimates of the corresponding values for monodentate formate. These values not only serve as important benchmarks for computational models, but also clarify the energetics of important elementary reaction steps that occur in catalysis on Cu surfaces.

2. EXPERIMENTAL METHODOLOGY

The experiments were performed in an ultrahigh vacuum (UHV) chamber (base pressure $<2 \times 10^{-10}$ mbar) designed for single-crystal adsorption calorimetry (SCAC). The chamber is also equipped with X-ray photoelectron spectroscopy (XPS), low-energy electron diffraction (LEED), Auger electron spectroscopy (AES), low-energy ion-scattering spectroscopy (LEIS), a quadrupole mass spectrometer (QMS), and a calibrated liquid-nitrogen-cooled quartz crystal microbalance (QCM), used to measure the absolute flux of the HCOOH molecular beam. The SCAC apparatus and experimental procedures for the molecular beam flux, sticking probability, and heat measurements have been described in depth previously.[2,37,38]

To briefly summarize, the Cu(111) sample used was a 2 μm thick single-crystal foil provided by Bine Hansen at Aarhus University. The surface was cleaned by repeated cycles of Ar^+ ion sputtering and annealing until a well-ordered (111) LEED pattern was obtained. (Due to the high reflectivity of Cu, the exact annealing temperature of the sample surface could not be determined using an optical pyrometer.) The oxygen-predosed surface was prepared by exposing the clean Cu(111) surface at 240 K to 30 L of O_2 gas (1 L = 1 Langmuir = 10^{-6} Torr sec), which we show below produces atomically adsorbed oxygen at a coverage of ∼0.10 ML O adatoms per Cu surface atom. The clean or O-predosed Cu(111) surface was exposed to a pulsed, collimated molecular beam of formic acid, and the heat of adsorption and sticking probability were recorded simultaneously. The purity of the HCOOH molecular beam generated in this way was verified with direct observation by the QMS, consistent with our earlier measurements.[6,13] The sticking probabilities (both long-term (S_∞) and short-term ($S_{102\ ms}$)) were measured with a QMS using the King and Wells method;[39] they are, as defined previously,[2,37] used to relate to the fraction of molecules in the gas pulse that stick to and remain on the surface until the start of the next pulse (S_∞) and those that stick long enough to contribute to the heat signal ($S_{102\ ms}$, which is measured only in the first 102 ms here). The heat of adsorption was measured by a pyroelectric ribbon pressed against the back of the Cu(111) crystal. The molecular beam was created by expanding approximately 4.0 mbar of formic acid through a glass capillary array held at 360 K and collimated through a series of orifices that are cooled with liquid nitrogen. The resulting molecular beam is then chopped into 102 ms pulses every 3 s.

Here, one monolayer of coverage is defined as the number of molecules of formic acid adsorbed to the surface per unit area, regardless of the product produced, normalized to the density of Cu atoms on the (111) surface (1.77×10^{19} atoms per m^2). A typical dose is 0.010 ML (∼4.5×10^{12} molecules within the beam diameter of ∼4 mm) per formic acid gas pulse.

Light pulses from a HeNe laser (632.8 nm) were used to calibrate the heat detector sensitivity, as described previously for studies on Pt(111)[1,2,5−8,10,40] and Ni(111).[3,4,12,13] Since Cu(111) has a much higher reported optical reflectivity for this wavelength (0.973)[41] than Pt (0.76) and Ni (0.65),[42] the accuracy of the laser calibration of the heat signal is less reliable than for Pt and Ni. (Any small relative difference between our samples' actual reflectivity and this literature value (which we assumed for calibration) leads to ∼10-fold larger error in the heat adsorbed.) These SCAC experiments on Cu also had ∼10-fold lower heat signal and poorer heat signal-to-noise ratio than was typical for experiments from this group on Pt and Ni. We think this may also be due at least partially to the much lower infrared optical emissivity (absorptivity) of Cu, which might make a large contribution to the heat transfer rate from the metal crystal to the heat detector. However, during the course of these measurements reported here, there was also an extra contribution to the heat signal's noise that was only discovered *after* the experiments reported here, so the signal-to-noise ratio on heats reported here is significantly lower than is in principle possible with the instrumentation used here even for Cu.

https://doi.org/10.1021/acscatal.2c02608
ACS Catal. 2022, 12, 10950−10960

3. RESULTS

3.1. Sticking Probabilities. Recent experiments have shown that formic acid will not dissociatively adsorb on clean Cu(111) except to a small extent attributed to the step edge defect density.[20,43] This produces low coverages of adsorbed formate, which takes on the monodentate structure ($HCOO_{mono,ad}$) at low temperatures but converts to bidentate ($HCOO_{bi,ad}$) at 200 K and above.[20,43] Higher coverages of monodentate formate can be formed by extended HCOOH gas dosing (10 to 30 min) at 150−160 K.[44] Early reports of rapid dissociative adsorption of HCOOH on Cu(111)[45,46] may have been due to X-ray beam damage.

Dissociative adsorption of HCOOH does occur rapidly on oxygen-predosed Cu(111), resulting in the formation of adsorbed formate in the bidentate structure, $HCOO_{bi,ad}$, with coverages up to 0.33 formate molecules per Cu surface atom.[47] That reaction was characterized at 330 K by the net stoichiometry:[47]

$$2HCOOH_g + O_{ad} \rightarrow 2HCOO_{bi,ad} + H_2O_g \quad (1)$$

However, this probably involves the step:

$$HCOOH_g + O_{ad} \rightarrow HCOO_{bi,ad} + OH_{ad} \quad (2)$$

which is known to occur on Cu(110) and Cu(111),[48,49] and then the two hydroxyls thus produced convert to water and O_{ad} via:

$$2OH_{ad} \rightarrow H_2O_g + O_{ad} \quad (3)$$

Reaction 3 is known to occur on Cu(111) already at 160 K during TPD after producing OH_{ad} by dosing methanol to a surface at 110 K with preadsorbed O_{ad}.[50] Interestingly, reaction 3 only occurs at much higher temperatures on the other widely studied Cu faces: 220 K on Cu(100)[51] and 290 K on Cu(110).[52,53] We note that reaction 2 above may occur in two steps, whereby the less stable monodentate formate forms first but converts to bidentate formate (as noted in literature cited farther above).

Given these results from the literature, one expects that when we dose HCOOH to O predosed Cu(111) at 240 K, we get the same net reaction as reaction 1.

Figure 1 shows the average long-term (S_∞) and short-term ($S_{102\ ms}$) sticking probabilities versus coverage for formic acid adsorption on O-predosed Cu(111) at 240 K. The HCOOH-derived coverages reported throughout this paper represent the amount of formic acid adsorbed for the entire duration of the experiment, regardless of the product produced (i.e., formate or molecularly adsorbed HCOOH). We will use "O-predosed Cu(111)" throughout to refer to a Cu(111) surface with ∼0.10 ML of oxygen adatoms, obtained by predosing 30 L of O_2 at 240 K. The long-term sticking probability (S_∞) is the probability that a gas molecule strikes the sample surface, sticks, and remains until the next gas pulse starts 3 s later. This is used to calculate the adsorbate coverage at the start of the next gas pulse. The short-term sticking probability ($S_{102\ ms}$) is the probability that a gas molecule strikes the sample surface, sticks, and remains at least through the time window of the heat measurement (i.e., the first 102 ms). This is used to calculate the number of moles of gas-phase reactants that contribute to the measured heat signal for that gas pulse and thus the heat of adsorption per mole adsorbed.

At 240 K, both the long-term and short-term sticking probabilities are initially high (>0.9) and remain at unity

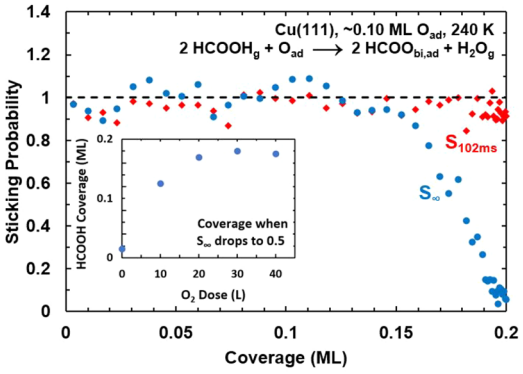

Figure 1. Average short-term (red diamonds, $S_{102\ ms}$) and long-term (blue circles, S_∞) sticking probabilities of formic acid dissociatively adsorbing on Cu(111) at 240 K, predosed with 0.10 ML O_{ad}, as a function of the HCOOH-derived adsorbate coverage. Note that the first red diamond with $S_{102\ ms}$ = 0.98 is nearly completely hidden under the first blue circle. A coverage of 1 ML is defined as one adsorbate per Cu(111) surface atom or 1.77×10^{19} $HCOO_{bi,ad}$ per m^2. Inset: The HCOOH-derived adsorbate coverage at which S_∞ at 240 K drops to 0.50 (which closely tracks its saturation coverage) versus the pre-exposure of O_2 gas to clean Cu(111) at 240 K.

(within the noise) through a coverage of ∼0.15 ML. Past this coverage, the long-term sticking probability drops off rapidly, reaching zero by 0.20 ML, while the short-term sticking probability remains high (>0.90). After this coverage, formic acid continues to transiently adsorb on the saturated adlayer with a high probability, as evidenced by the high short-term sticking probability, but desorbs again completely (but slowly) before the next pulse starts 3 s later. This suggests that the O adatoms are fully reacted in the dissociative adsorption reaction, and no further dissociative adsorption can occur. We note that the temperature here is above that necessary for multilayer adsorption (∼150 K[43]), so no molecular adsorption beyond the first layer is expected.

The inset in Figure 1 shows the HCOOH coverage at which its long-term sticking probability at 240 K drops to 0.50 (which closely tracks the saturation coverage of dissociatively adsorbed HCOOH) as a function of the amount of pre-exposure of the clean Cu(111) surface at 240 K to O_2 gas. As seen, this HCOOH coverage increases steeply with O_2 predose, from nearly zero with no predose of O_2, and quickly saturates at ∼0.18 ML after ∼20 L of O_2. Similarly, the HCOOH coverage at which its S_∞ dropped below 0.1 saturated at ∼0.20 ML after ∼20 L of predosed O_2 (not shown). Assuming a 2:1 stoichiometric ratio in reaction 1 proposed above based on prior literature ($2HCOOH_g + O_{ad} \rightarrow 2HCOO_{bi,ad} + H_2O_g$), we take this to indicate that the 30 L O_2 pre-exposure at 240 K used in Figure 1, which gives a saturation formate coverage of 0.20 ML, corresponds to about 0.10 ML of O adatoms. This is about 10-fold smaller O_2 dose than was reported to produce this same coverage on Cu(111) at a higher temperature (296 K).[54] This coverage of O_{ad} is also smaller than the saturation coverage at 296 to 600 K (reported as ∼0.44 ML[54]). Defects such as step edges may aid in O_2 dissociation, especially at the lower temperature used here.

Based on the prior literature summarized above, we concluded that when we dose HCOOH to O-predosed Cu(111) at 240 K, we get the same net reaction as reaction 1. This also means that gaseous H_2O should have evolved simultaneously with the dissociation of HCOOH. We

https://doi.org/10.1021/acscatal.2c02608
ACS Catal. 2022, 12, 10950−10960

attempted to detect this H_2O_g by averaging the QMS signal at m/e = 18 for the pulses below 0.2 ML dose, but were unable to see signal above the noise due to H_2O evolution. However, given the high background signal of water in the chamber (and associated large noise at m/e = 18), the expected water peak intensity (~1/2 the QMS signal for formic acid at zero-sticking probability, according to the stoichiometry of reaction 1) would not have been visible above the noise in the background signal. Thus, we still believe reaction 1 dominates at 240 K.

At 120 K on clean Cu(111), where formic acid adsorbs molecularly, the short-term and long-term sticking probabilities are both unity (within the pulse-to-pulse noise similar to that in Figure 1) at all coverages, so they are not shown here. As this temperature is low enough to form multilayers of formic acid on the Cu(111) surface, the sticking probability was found to remain at unity through at least five layers of coverage.

3.2. Heats of Adsorption. In this paper, the term "heat of adsorption" is defined at the negative of the standard molar enthalpy change for the adsorption reaction, with the gas and the sample surface being at the sample temperature. As explained in detail previously, this requires a small enthalpy correction on the measured heat since the gas molecule's enthalpy in the molecular beam is slightly higher than in a Boltzmann distribution at the Cu(111) temperature due to the actual experimental molecular beam conditions.[2] The differential heat of adsorption is the heat released per mole when a small increment of adsorbate is added to the surface at nearly fixed coverage, as occurs in one of our molecular beam pulses during SCAC. The integral heat of adsorption is the integral of the differential heat versus coverage from zero up to the coverage of interest, divided by that coverage, and is thus the average heat for that coverage range.

Figure 2 shows the differential heats of adsorption for formic acid on clean Cu(111) at 120 K (blue) and on O-predosed Cu(111) at 240 K (red) (after this small correction to the raw heats noted above) as a function of adsorbate coverage. The integral heat of adsorption at 240 K is also shown in black from the low coverage limit. These are averages of three and nine runs at 120 and 240 K, respectively. For both the 120 and 240 K data, the first two data points are significantly higher than subsequent points and are attributed to adsorption on defect sites on the surface, likely at step edges. These two points are excluded from integral heat and initial heat determinations so that these values correspond to adsorption on terraces and are not inclusive of these defect sites that bind more strongly.

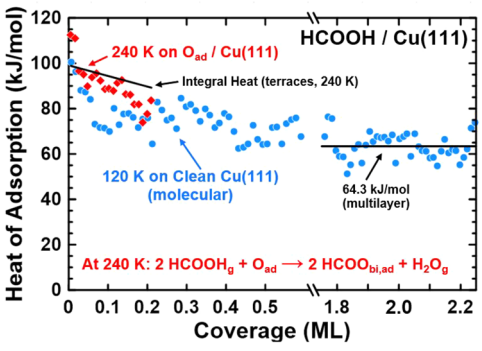

Figure 2. Differential heats of adsorption of formic acid on clean Cu(111) at 120 K (blue circles) and O-predosed Cu(111) at 240 K (red diamonds) as a function of the HCOOH-derived adsorbate coverage. The average heat of molecular adsorption at the multilayer limit is shown by the black line through the 120 K data, giving 64.3 ± 2.9 kJ/mol. The integral heat of adsorption for 240 K is shown from the low coverage limit as the black-line fit (99.1−46.8θ) kJ/mol, giving 89.7 kJ/mol at saturation (θ = 0.20 ML). One ML = 1.77 × 10^{19} adsorbates per m^2.

Previous results from literature show that formic acid molecularly adsorbs on clean Cu(111) below ~250 K, and multilayers will adsorb to the surface below 150 K.[43] Thus, calorimetric measurements at 120 K on clean Cu(111) correspond to molecular adsorption of formic acid in the first layer, with the formation of multilayers at higher coverages.

At 120 K, the initial heat of adsorption is 80.9 kJ/mol (excluding the first two points, which are higher, and may be due to adsorption at defects, likely step edges). The heat decreases approximately linearly with coverage until reaching ~70 kJ/mol by 0.50 ML, where the first adlayer of formic acid appears to be completed. A very similar decrease (~10 kJ/mol) in heat of HCOOH adsorption with coverage was reported on Pt(111) and Ni(111),[6,13] implying net repulsive adsorbate−adsorbate interactions. The HCOOH units are likely attached by hydrogen bonds, but groups of H-bonded HCOOHs must have group−group repulsions. This has been suggested to occur for methanol on Pt, Au and Cu(111),[55] where H-bonded hexamers and/or chains have repulsive group−group interactions. Beyond 0.5 ML, the heat of adsorption stays constant at ~68.5 kJ/mol through ~1.5 ML, before decreasing to the multilayer energy value of 64.3 ± 2.9 kJ/mol. (This is the run-to-run average and standard deviation of the multilayer heats of the three runs.) Each run's multilayer heat is the pulse-to-pulse average heat for coverages above 1.75 ML. The heat of sublimation of bulk formic acid was estimated to be 61.9 kJ/mol at 120 K, using literature values for the enthalpies of phase transitions[56] along with heat capacities of solid, liquid, and gaseous formic acid,[57] as a heat of sublimation at 120 K was not available in literature. The bulk heat of sublimation at 120 K was also estimated using the same heat capacities but instead starting from a reported bulk heat of sublimation at 200 K (60.5 kJ/mol[58]), which gives a very similar value of 61.3 kJ/mol. The average of these two bulk literature values (61.3 and 61.9 kJ/mol) falls within the error bars of the multilayer heat measured here (61.4−67.2 kJ/mol). This close agreement provides an estimate of the absolute accuracy of the results in Figure 2. The ~2 kJ/mol higher heat of adsorption in the first monolayer after completion of the first adlayer (i.e., between 0.5 and 1.5 ML coverage) is possibly due to long-range attractive interactions between HCOOH molecules and the underlying metal (e.g., dipole−induced dipole interactions). It is common to have higher heats than the true multilayer heats in the layer after completion of the first adlayer.[1,59,60]

At 240 K, the initial heat of adsorption on the O-predosed Cu(111) surface is 99.1 kJ/mol (again excluding the first two points, which are higher, and may be due to adsorption at defects, likely step edges). The heat decreases approximately linearly with coverage until reaching 80.4 kJ/mol by a coverage of ~0.20 ML. Past this point, the long-term sticking probability has dropped to zero, indicating that surface O adatoms have been fully consumed by the dissociation reaction and the surface adlayer is saturated. Any additional formic acid molecules that impinge on the surface adsorb transiently (as indicated by the high short-term sticking probability), but fully desorb before the next pulse begins 3 s later. The integral heat

https://doi.org/10.1021/acscatal.2c02608
ACS Catal. 2022, 12, 10950−10960

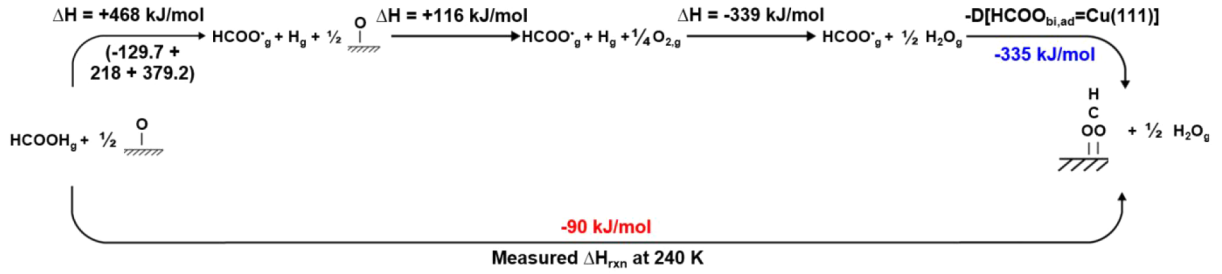

Figure 3. Thermodynamic cycle used to determine the total bond enthalpy of bidentate formate to Cu(111) (formate gas to surface-bound bidentate formate) from the *integral* heat of dissociative formic acid adsorption at 240 K and 0.20 ML of formate (90 kJ/mol, shown in red). The top right-hand step shows the enthalpy to form bidentate formate from gas-phase formate radical, which provides an estimate of the total bond enthalpy of bidentate formate to Cu(111), from both its O−Cu bonds. Values in red are experimental values from this study, black are taken from literature as described in the text, and blue values are values that were extracted using this cycle.

of adsorption at 240 K is shown in black versus coverage up to saturation and is well fit by $(99.1-46.8\theta)$ kJ/mol, where θ is coverage in ML, with an integral heat of 89.7 kJ/mol at saturation (0.20 ML).

Above saturation on O-predosed Cu(111) at 240 K, the transiently adsorbed HCOOH has a constant heat of adsorption at saturation ($\Delta H_{ad,sat}$) of 72.5 ± 3.3 kJ/mol. By averaging the mass spectrometry pulse line-shapes (signal versus time) after saturation and fitting an exponential decay function to the postpulse signal decay, we obtained a decay constant, τ, which is equal to the reciprocal of the first-order desorption rate constant, k_{des}, given by[61]

$$1/\tau = k_{des} = \nu_{des}\exp(-E_{des}/RT) \quad (4)$$

where ν_{des} is the prefactor for desorption, E_{des} is the activation energy of desorption, R is the gas constant, and T is the temperature. Using the values of τ = 0.85 s and k_{des} = 0.173 s^{-1} determined from this exponential decay fit, along with E_{des} = 71.5 kJ/mol determined from the measured heat after saturation ($E_{des} = \Delta H_{ad,sat} - 1/2RT$[62]), a prefactor for desorption can be calculated. In that way, we determined an experimental prefactor for HCOOH desorption of $\nu_{des} = 4.3 \times 10^{15}$ s^{-1}. This can be compared to the prefactor for desorption estimated by the method of Campbell and Sellers,[61] which gives $\nu_{des} = 2.4 \times 10^{15}$ s^{-1} for molecularly adsorbed HCOOH at 240 K. This good agreement indicates that the transiently adsorbed HCOOH is molecularly adsorbed and not, for example, transiently dissociated and then recombined.

4. DISCUSSION

4.1. Energetics of Adsorbed Formate on Cu(111) at 240 K. As discussed above, our calorimetric measurements on the O-predosed Cu(111) surface at 240 K represent the heats of dissociative formic acid adsorption onto Cu(111), via reaction 1 above: $2HCOOH_g + O_{ad} \rightarrow 2HCOO_{bi,ad} + H_2O_g$. By using available literature values for the heats of formation of various gas-phase and adsorbed molecules and the experimentally measured heat at 240 K, we can extract the bond enthalpy of bidentate formate to Cu(111) ($HCOO_{bi,ad}$=Cu(111)) and the enthalpy of formation of bidentate formate on the Cu(111) surface ($\Delta H_f(HCOO_{bi,ad})$). To do so, we construct the thermodynamic cycles shown in Figure 3 and Figure 4. Note that all positive heats of adsorption in Figure 2 represent exothermic processes, while here they have been converted to negative enthalpies of reaction for use in the thermodynamic cycles.

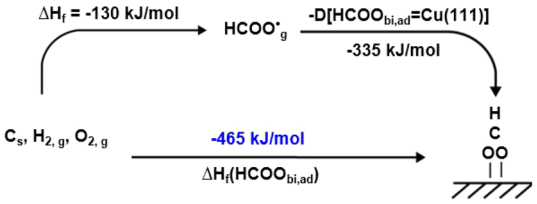

Figure 4. Thermodynamic cycle used to determine the total enthalpy of formation of bidentate formate on Cu(111) using the total bond enthalpy extracted from the thermodynamic cycle above (Figure 3). The bottom pathway shows the total enthalpy to form surface-bound bidentate formate from elements in their standard states. Values in black are previously extracted values or tabulated enthalpies of formation as referenced in the text, and blue values are values that were extracted using this cycle.

The cycle in Figure 3 begins on the left-hand side, starting with gas-phase formate and a surface-bound oxygen atom (but with only 1/2 mol of O_{ad}, for 1/2 of the stoichiometry of reaction 1, which then corresponds to a single formate adsorbate). The bottom pathway represents our measurement at 240 K and is quantified by the integral heat of adsorption at 0.20 ML. This must be energetically equivalent to the parallel pathway; therefore, the sum of the steps in the top pathway must equal −90. kJ/mol. The first step in the top pathway is to dissociate gas-phase formic acid into a gas-phase hydrogen atom and a gas-phase formate radical. The enthalpy of reaction for this step (+468 kJ/mol) is calculated using literature values for the enthalpies of formation for each of the three gas-phase species from elements in their standard states at 298 K ($HCOOH_g$ = −379.2, $HCOO_g$ = −129.7, and H_g = +218.0, in kJ/mol).[56]

In the second step of the top pathway, the 1/2 oxygen adatom is desorbed to form 1/4 gaseous O_2, with the other species unchanged. In the absence of any reported value for the enthalpy of formation of adsorbed O on Cu(111), or the reverse of this step, the enthalpy of this reaction (+116 kJ/mol) is estimated from reported literature values for the enthalpy of dissociative adsorption of O_2 on polycrystalline Cu of 465 kJ per mole O_2.[63,64] Reported DFT calculations (summarized in Table 3 below) for the adsorption energy of O_{ad} on different Cu faces showed that O_{ad} is 21 to 36 kJ/mol less stable on Cu(111) than on the (110) and (100) faces.[65] This suggests that this calorimetric heat for 1/2 O_{ad} → 1/4 $O_{2,g}$ of 116 kJ/mol in Figure 3 may be too large for Cu(111) by 10 to 18 kJ/mol. The third step in the top pathway is to combine O_2 gas and H gas to form gaseous water. The

https://doi.org/10.1021/acscatal.2c02608
ACS Catal. 2022, 12, 10950−10960

Table 1. Comparison of the Present Calorimetric Bond Energies of Bidentate and Monodentate Formate to the Cu(111) Surface with Calculated Values Using DFT

coverage	DFT functional or method	$HCOO_{bi,ad}$ bond energy (kJ/mol)	$HCOO_{mono,ad}$ bond energy (kJ/mol)	ref
0.20 ML (1/5 ML)	calorimetry	333−315	305−287	this paper
0.11 ML (1/9 ML)[a]	calorimetry	337−319	309−291	this paper
DFT:	–	–	–	–
0.11 ML (1/9 ML)	RPBE	242	200	31
0.11 ML (1/9 ML)	PBE-DFT-D2	253	218	30
0.11 ML (1/9 ML)	PW91 /	268, 266 /	217 /	17,32
	(PW91 with ZPE)	(253)	(206)	
0.25 (1/4 ML)	GGA-PW91 /	267 /	224 /	15
	(GGA-PW91 with ZPE)	(253)	(210)	

[a]As many DFT values reported here are calculated at 0.11 ML coverage, the experimentally determined bond enthalpy values of bidentate and monodentate formate to Cu(111) were also calculated at 0.11 ML in an identical manner to that at 0.20 ML but using the integral heat value at 240 K and 0.11 ML of 94 kJ/mol.

enthalpy of this step (−339 kJ/ml) was calculated using literature values for the enthalpies of formation for each of the three gas-phase species from elements in their standard states at 298 K.[56]

Finally, this leaves the top right step as the only unsolved value. This step represents the enthalpy to form bidentate formate from the gas-phase formate radical, which provides an estimate of the total bond enthalpy of bidentate formate to Cu(111), from both its O−Cu bonds. The extracted $HCOO_{bi,ad}$=Cu(111) bond enthalpy is 335 kJ/mol. Given that this value is very close to that of the bond enthalpy of bidentate formate to Ni(111) (320 kJ/mol[13]), we assume the same difference in bond enthalpies between mono- and bidentate formate on Cu(111) as previously measured on Ni(111) (28 kJ/mol[13,66]) in order to estimate the bond enthalpy of monodentate formate to Cu(111). This estimated bond enthalpy of monodentate formate to Cu(111), or $HCOO_{mono,ad}$-Cu(111), is thus 335−28 = 307 kJ/mol. This assumed difference between mono- and bidentate formate of 28 kJ/mol is also close to that calculated on Cu(111) by DFT (42 kJ/mol[15]) and that measured on Pt(111) (33 kJ/mol[6,66]). Since the 1/2 O_{ad} species on Cu(111) may be up to 18 kJ/mol less stable than the enthalpy value used for 1/2 O_{ad} in this cycle of Figure 3 (which is for polycrystalline Cu instead of Cu(111), see above), these bond enthalpies of both bi- and monodentate formate to Cu(111) may be smaller by up to 18 kJ/mol, placing them very close to their values to Ni(111).

Figure 4 shows how this extracted $HCOO_{bi,ad}$═Cu(111) bond enthalpy can be used in another thermodynamic cycle to extract the enthalpy of formation of bidentate formate on Cu(111). In this case the cycle starts on the left-hand side with the elements in their standard states. The top pathway uses first the literature value for the enthalpy of formation of gas-phase formate,[67] followed by the extracted bond enthalpy of bidentate formate from Figure 3. This results in the formation of surface-bound bidentate formate. The bottom pathway then represents the enthalpy of formation for bidentate formate on Cu(111), and again must be energetically equivalent to the parallel pathway. The resulting extracted value for the enthalpy of formation of bidentate formate, or $\Delta H_f(HCOO_{bi,ad})$, on Cu(111) is −465 kJ/mol. Using the same method as discussed above, the estimated corresponding enthalpy of formation for monodentate formate, or $\Delta H_f(HCOO_{mono,ad})$, on Cu(111) is −465 + 28 = −437 kJ/mol. Again, these heats of formation of both bi- and monodentate formate to Cu(111) may be smaller in magnitude (less stable) by up to 18 kJ/mol.

4.2. Comparison of Calorimetric Energy of Adsorbed Formate and HCOOH to DFT. The bond energies of bidentate and monodentate formate to Cu(111) measured in this work are compared to theoretical values obtained by DFT in Table 1. DFT calculations report integral bond energies of adsorbates at specific coverages. Bond enthalpies were converted to bond energies by subtracting RT (2 kJ/mol at 240 K). The bidentate bond enthalpies at 0.20 ML were calculated from the thermodynamic cycle in Figure 3. In order to match the reported coverage of most of the DFT values, equivalent values at 0.11 ML were calculated in an identical manner to that at 0.20 ML, but using the integral heat value at 240 K and 0.11 ML of 94 kJ/mol. All of these values in Table 1 for Cu(111) show a range that extends to lower adsorbed formate stability by 18 kJ/mol to allow for the uncertainty in the calorimetric heat of formation of O_{ad} mentioned above.

As can be seen, all of the reported DFT calculations significantly underestimate the measured bond energies of bidentate and monodentate formate to the Cu(111) surface. On average, the DFT values are ∼80 to 62 kJ/mol lower than the experimentally determined bond energy of bidentate formate, and ∼95 to 77 kJ/mol lower than that for monodentate formate. While larger in magnitude for Cu(111), this underestimation of the formate bond energy by DFT is also seen when comparing the experimental and theoretical values for Ni(111). For example, prior DFT calculations had underestimated the bond energy of bidentate formate to Ni(111) by 26 to 58 kJ/mol compared with calorimetry.[13] Both of these margins of error are supported by the fact that it is well-known that DFT has substantial errors in energy accuracy.[68] Since prior to this present work, there had not been experimentally determined bond energies reported for *any* molecular fragment on *any* well-defined Cu surface, this work provides an important benchmark for comparison to computational studies of small molecular fragments on Cu(111). However, future experimental results beyond the formate/Cu(111) system will be important for extending these benchmarks to Cu systems more widely.

A PW91 DFT study calculated the adsorption energy of HCOOH on Cu(111) to be 15 kJ/mol,[19] compared with the integral heat of molecular adsorption of ∼80 kJ/mol found here by calorimetry.

4.3. Comparison of Adsorbed Formate Energy on Cu(111) to Pt(111) and Ni(111). Previous calorimetric measurements by this group studied the adsorption of formic acid on Pt(111) and Ni(111), allowing for a direct comparison

https://doi.org/10.1021/acscatal.2c02608
ACS Catal. 2022, 12, 10950−10960

Table 2. Comparison of Calorimetrically Measured Enthalpies of Formation and Bond Enthalpies of Monodentate and Bidentate Formate on Pt(111), Ni(111) and Cu(111). Also Listed Are DFT (PW91) Bond Energies for Bidentate Formate at 1/9 ML

	coverage (ML)	ΔH_f $HCOO_{mono,ad}$ (kJ/mol)	ΔH_f $HCOO_{bi,ad}$ (kJ/mol)	bond enthalpy $HCOO_{mono,ad}$ (kJ/mol)	bond enthalpy $HCOO_{bi,ad}$ (kJ/mol)	bond enthalpy $HCOO_{bi,ad}$ (by DFT, kJ/mol)
Pt(111)	0.25	−345 (ref 62)	−381 (ref 62)	221 (ref 66)	251 (ref 62)[a]	227 (refs 32,69)
Ni(111)	0.143[b]	−422 (ref 13)[c]	−449 (ref 13)	292 (ref 66)	320 (ref 13)	270 (ref 32)
Cu(111)	0.20	−(437−419)	−(465−447)	307−289	335−317	266 (ref32)

[a]The bond enthalpy of bidentate formate to Ni(111) was calculated from this listed enthalpy of formation of bidentate formate on Ni(111) using the known heat of formation of formate gas (−129.7 kJ/mol[56]). [b]Values for monodentate formate on Ni(111) were reported at 0.20 ML, while the other values are at 0.143 ML. [c]This enthalpy of formation of monodentate formate on Ni(111) was calculated from this listed bond enthalpy of monodentate formate to Ni(111) (292 kJ/mol,[66] estimated from calorimetry data measured previously[13]), using the known heat of formation of formate gas (−129.7 kJ/mol[56]).

between the three metal surfaces.[6,13] The values of the bond enthalpies and enthalpies of formation for both mono- and bidentate formate to Pt(111), Ni(111), and Cu(111) are summarized in Table 2. When possible, coverages as close to the saturation coverage of 0.20 ML in this work are listed here, but that is not available for all values. The bidentate formate bond enthalpies are 251, 320, and 335 to 317 kJ/mol on Pt(111), Ni(111), and Cu(111), respectively. The enthalpies of formation of bidentate formate are −381, −449, and −(465 to 447) kJ/mol on Pt(111), Ni(111), and Cu(111), respectively. Thus, the formate bond energies to Cu(111) are experimentally indistinguishable from those to Ni(111) but 68 to 84 kJ/mol stronger than to Pt(111).

These calorimetric bond energies for monodentate formate to Pt(111) and Ni(111) were well fitted based on a model previously developed by Carey and Campbell that is based on Pauling's equation and uses only known parameters (gas-phase ligand-hydrogen bond enthalpies, bond enthalpies of adsorbed H atoms to the surface, electronegativities of the elements, and group electronegativities).[66] That model explained well the much stronger formate bond energies to Ni(111) compared with Pt(111), mainly associated with their differences in electronegativity. The electronegativity of Cu is much closer to that for Ni than Pt, suggesting that formate could have bond energy of Cu(111) similar to Ni(111). However, that model also includes a term for the H atom's bond energy to the surface, which is much stronger for Ni(111) than Cu(111) and would predict formate to bind more strongly to Nui than Cu. Indeed, that model was also used to predict formate bond energies to surfaces for which experimental measurements had not yet been reported, including Cu(111). The model's predicted bond enthalpy of monodentate formate to Cu(111) was 228 kJ/mol,[66] versus the estimated experimental value of 307 to 289 kJ/mol reported here. This is a large error but slightly smaller than DFT errors (see above). This model also predicted the bond enthalpy of monodentate formate to Ni(111) (275 kJ/mol) to be a lot stronger than to Cu(111) (228 kJ/mol), whereas the experiments show these to be similar or with Cu(111) stronger.

Table 2 also lists the bond energies for bidentate formate to these three metal surfaces as reported from DFT calculations (using the same version of PW91 at the same coverage by the same group in all cases).[32,69] (These DFT energies are without ZPE correction, but that correction would lower these bond energies by nearly the same ∼14 kJ/mol on all three metals.) As seen, DFT has reproduced the experimental observations that formate binds much more weakly to Pt(111) than to Ni(111) or Cu(111), while the bond energies to Ni(111) and Cu(111) are much closer to each other. Still, the errors in DFT relative to SCAC are rather large (−24, −50 and −(69 to 51) kJ/mol for Pt, Ni, and Cu(111), respectively.) It is well-known that DFT has substantial errors in energy accuracy in comparison to experimental energies, but these present errors are somewhat larger than the mean absolute error of 28 kJ/mol reported for PW91 on a group of 25 such "strongly covalently adsorbed" systems, which showed a mean signed error of −20 kJ/mol.[68] If one adds 48 kJ/mol uniformly to all three of these PW91 bond energies, their errors relative to experiments drop to only +24, −2, and −(21 to 3) kJ/mol for Pt, Ni, and Cu(111), respectively. This suggests there might be some large (∼48 kJ/mol) error in DFT for the energy of the reference state for all of these bond energies: gaseous formate radical. In addition, it is known that PW91 underestimates adsorption energies by ∼40 kJ/mol on average for systems where van der Waals interactions are thought to contribute a large amount to the adsorption energy.[68] Again, this present work on Cu(111) provides an important benchmark to aid future efforts to improve computational accuracy for adsorbate energies on late transition metals.

Further experimental measurements of molecular fragments on Cu(111) will be important to validate this observed difference between the experimental values measured here and those predicted by DFT or the electronegativity-based model of Carey and Campbell. At this point the basis for this difference is unclear, and the study of additional oxygenates on Cu might further elucidate the underlying reasons.

4.4. Adhesion Energy of Liquid Formic Acid to Cu(111). Solvent/metal adhesion energies are crucial to understanding solvent effects on adsorption energies, which is increasingly critical as catalytic and electrocatalytic reactions occurring at solid surfaces in liquid solvents become more important. The determination of the adhesion energy for liquid formic acid on Cu(111) can provide valuable insight into the energetics of this liquid−solid interface. However, there is currently no way to directly measure the adhesion energy of a liquid solvent to a clean metal surface. To estimate this adhesion energy, we will employ a recently developed method from this group that allows for an estimate of the adhesion energy from experimentally determined differential heat of adsorption data like that in Figure 2.[70,71] See refs 1,70, and 71 for an in-depth derivation and discussion of this model.

This model results in the following equation for the determination of adhesion energy from calorimetric data:

$$E_{adh,S(liq)/M(s)} = [Q_{adsorption} - n\cdot\Delta H_{vap,S}]/A + 2\gamma_{S(liq)} \quad (5)$$

https://doi.org/10.1021/acscatal.2c02608
ACS Catal. 2022, 12, 10950−10960

where $E_{adh,S(liq)/M(s)}$ is the adhesion energy of the liquid solvent (formic acid) to the solid metal surface (Cu(111)), $\gamma_{S(liq)}$ is the surface energy per unit area of bulk, liquid formic acid, and the term $[Q_{adsorption} - n{\cdot}\Delta H_{vap,S}]/A$ is equal to the numerically integrated area from zero coverage up to a (bulklike) multilayer coverage (with n moles adsorbed per area A) of the heat versus coverage curve ($Q_{adsorption}$) minus n/A times the molar heat of vaporization of the liquid solvent ($\Delta H_{vap,S}$). Ideally, these values would all be measured at room temperature to provide the adhesion energy at room temperature. Since $Q_{adsorption}$ can only be measured on a clean metal surface in ultrahigh vacuum, which is only possible for formic acid at temperatures where the solvent grows as solid films rather than liquid films, the assumption was made that the term $[Q_{adsorption} - n{\cdot}\Delta H_{vap,S}]/A$ at room temperature is approximately equal to the analogous quantity at experimental temperatures where the solvent is a solid, or $[Q_{adsorption} - n{\cdot}\Delta H_{sub,S}]/A$, where $\Delta H_{sub,S}$ is the heat of sublimation of bulk formic acid.

Using this method and the reported surface energy of bulk, liquid formic acid of $\gamma_{S(liq)} = 0.0377$ J/m^2,[71,72] we calculate the adhesion energy of liquid formic acid to the Cu(111) surface at 120 K to be $E_{adh} = 0.271$ J/m^2. Comparatively, this value is slightly less than the adhesion energy of formic acid to Ni(111) (0.279 J/m^2) but greater than that to Pt(111) (0.162 J/m^2).[71]

Understanding this adhesion energy, and particularly how it compares to other common solvents, could enable the intelligent selection among these solvents to tune reaction environments to have more desirable energetics for surface adsorption or desorption for catalytic reactants and intermediates. Unfortunately, there is currently no other reported solvent adhesion energies to the Cu(111) surface for comparison. However, these values are reported for multiple solvents on Pt(111) and Ni(111) and follow the trend of methanol < formic acid < water < benzene ≈ phenol.[71] This indicates that solvents with higher heats of adsorption per unit area in the first adsorbed layer have higher adhesion energies to a given metal surface. We note that these adhesion energies were all estimated using the same assumption of a negligible difference in heat capacities (including the heat of fusion) between the first and subsequent layers, and the errors associated with this assumption are possibly large (~25%). However, all of these errors are likely qualitatively similar, so these trends in E_{adh} values will remain. The close alignment of the adhesion energy of liquid formic acid to Cu(111) with the equivalent values to Pt(111) and Ni(111) suggests that these energetic trends will extend to the Cu(111) surface as well. However, further experimentally determined solvent/metal adhesion energy values on Cu(111), along with computational approaches, will provide valuable comparison to support or refute the extension of these trends to Cu(111).

4.5. Formic Acid Multilayer Structure on Cu(111). The multilayer heat of adsorption obtained in this work on Cu(111) (64.3 ± 2.9 kJ/mol) is in close agreement with the estimated range for the heat of sublimation of bulk formic acid of 61.3−61.9 kJ/mol at 120 K, estimated from literature values as noted above. However, this is different than those heats previously reported by this group for multilayer adsorption of formic acid on Pt(111) and Ni(111) (49.9 and 52.8 kJ/mol, respectively).[6,13] Previous literature results show that below 143 K, adsorption of formic acid on Pt(111) results in the formation of an amorphous multilayer rather than the more stable crystalline (also referred to as polymeric) phase.[73,74] Therefore, Silbaugh et al. attributed the observed multilayer heat of 49.9 kJ/mol measured at 100 K to amorphous multilayer adsorption on Pt(111).[6] However, infrared adsorption reflection spectroscopy studies of formic acid multilayers on Cu(111) at 100 K indicate that it is a polymeric (crystalline) phase when grown instead on Cu(111).[20] This crystalline phase is expected to be more stable than the amorphouse phase seen on Pt(111), as supported by the higher multilayer heat of adsorption seen here on Cu(111). Therefore, this multilayer heat measured at 120 K in Figure 2 is assigned to a crystalline phase. Imaging with STM of monolayer formic acid molecularly adsorbed on Cu(111) also shows a crystalline phase in the first layer between 80 and 120 K,[43] which may act as a template to enable crystalline growth in the multilayer. This first-layer polymeric phase on Cu(111) is composed of hydrogen-bonded chains that align in a β configuration on the surface (roughly a zigzag structure) that minimizes repulsive forces,[43] and is consequently likely to be more energetically favorable than amorphous adsorption.

4.6. Stability of OH_{ad} and Energetics of H_2O Desorption on Cu(111), Cu(100), and Cu(110). In analyzing the heat measurements above when making bidentate formate, we used the fact that the desorption temperature for H_2O_g from $2OH_{ad} \rightarrow H_2O_g + O_{ad}$ (reaction 3) was reported in a study of the dissociative adsorption of methanol on O-dosed Cu(111)[50] to be 160 K, so that this process was fast at our measurement temperature of 240 K. However, this temperature of 160 K is much lower than that known for this same reaction on Cu(110) (290 K[52,53]). To our knowledge, such a large percentage change in desorption temperatures between low-index faces of the same metal has not been reported for any reaction. As this value of 160 K for Cu(111) was only reported by one group, we wanted to verify that it is reasonable. To do this, we next compare this experimental difference to predicted results extracted from adsorption energies for O_{ad}, OH_{ad}, and H_2O_{ad} on Cu(111), Cu(100), and Cu(110) calculated by DFT.[65] The DFT adsorption energies used for these calculations, along with resulting enthalpies of reaction and predicted desorption temperatures are summarized in Table 3. To get these, we used the energy for the gas-phase reaction $2OH_g \rightarrow H_2O_g + O_g$ to be −70.7 kJ/mol as calculated from the experimental standard heats of formation of O_g, OH_g, and H_2O_g reported at 298 K (249.1, 39.0, and −241.8 kJ/mol, respectively).[56]

The listed adsorption energies were first used to calculate the enthalpy of reaction for reaction 3 (the desorption of gaseous water via $2OH_{ad} \rightarrow H_2O_g + O_{ad}$). This resulting reaction enthalpy was converted to an activation energy for water desorption energy by this reaction, E_{des}, by subtracting 1/2 RT. We made the assumption that this net reaction's enthalpy was equal to its activation energy (after converting from enthalpy to energy) based on computational results in literature that predict that the energetic barrier for desorption of molecularly adsorbed water is far larger than the energetic barrier for the reaction of two surface-bound hydroxyls to form adsorbed water plus O_{ad} on Cu(111).[15] Table 3 also shows that the DFT energy for reaction 3 is considerably more endothermic than that for the reaction $2OH_{ad} \rightarrow H_2O_{ad} + O_{ad}$. Thus, we assume that $2OH_{ad} \rightarrow H_2O_{ad} + O_{ad}$ is fast to equilibrium, followed by the slow step $H_2O_{ad} \rightarrow H_2O_g$, so that the net reaction 3 has an activation energy equal to the sum of the reaction energies those two elementary steps.

https://doi.org/10.1021/acscatal.2c02608
ACS Catal. 2022, 12, 10950−10960

Table 3. Summary of Adsorption Energies Taken from DFT and the Resulting Calculated Reaction Enthalpies and Predicted TPD Desorption Peak Temperatures for H_2O Desorption from Cu(111), Cu(100), and Cu(110), Compared to Published TPD Results[50]

crystal surface:	Cu(111)	Cu(100)	Cu(110)
$\Delta E_{ads,DFT}$ of OH_{ad} (kJ/mol) (ref 65)	−315	−389	−349
$\Delta E_{ads,DFT}$ of O_{ad} (kJ/mol) (ref 65)	−488	−524	−509
$\Delta E_{ads,DFT}$ of H_2O_{ad} (kJ/mol) (ref 65)	−21	−24	−37
$\Delta H_{rxn,DFT}$ for: $2OH_{ad} \rightarrow H_2O_g + O_{ad}$ (kJ/mol)	70	83	119
$\Delta H_{rxn,DFT}$ for: $2OH_{ad} \rightarrow H_2O_{ad} + O_{ad}$ (kJ/mol)	49	59	82
predicted T_{max} for H_2O desorption (K)	244	286	407
predicted T_{max} if $\Delta H_{rxn} = (0.70*\Delta H_{rxn,DFT})$ (K)	173	202	287
T_{max} from TPD (K) (ref 50)	160	220	290

A prefactor for desorption of $\nu_{des} = 5 \times 10^{14}$ s^{-1} was estimated using the method of Campbell and Sellers.[61] Together, these E_{des} and ν_{des} values can be used to estimate a temperature for the desorption of H_2O via the reaction 3 $OH_{ad} \rightarrow H_2O_g + O_{ad}$ from each of the three surfaces, using the first-order Readhead equation:[75]

$$E_{des} = RT_m[\ln(\nu_{des}T_m/\beta) - \ln(-E_{des}/RT_m)] \quad (6)$$

where R is the gas constant, T_m is temperature corresponding to the maximum of the desorption peak in TPD, and β is the heating rate. Using an assumed $\beta = 5$ K/s, the resulting estimated T_m values for Cu(111), Cu(100), and Cu(110) are 244, 286, and 407 K, respectively. In comparison, the values obtained in the TPD study of methanol by Pöllmann et al. are 160, 220, and 290 K, respectively.[50] As seen, the extremely wide range of the temperatures of desorption is reflected in the predicted temperatures, but the accuracy of the values are not well aligned with the experimental results. However, if we scale the DFT-derived reaction enthalpies by 0.70, equivalent to assuming an overestimation of the reaction enthalpy of ∼50% by DFT, we obtain desorption temperatures of 173, 202, and 287 K for Cu(111), Cu(100), and Cu(110). These values are now in very close agreement to the results of Pöllmann et al., and provide a verification of both the experimentally determined desorption temperatures and the extreme dependence of this temperature on the crystal face of Cu.

5. CONCLUSIONS

The energetics of the molecular and dissociative adsorption of formic acid on Cu(111) were measured by SCAC. The enthalpy of formation and bond enthalpy of bidentate formate to Cu(111) are −465 and 335 kJ/mol, respectively, at 240 K and 0.20 ML. Corresponding enthalpies are estimated for monodentate formate on Cu(111), which give an enthalpy of formation of −437 kJ/mol and a bond enthalpy of 307 kJ/mol. A comparison to DFT calculations in the literature shows that DFT systematically underestimated the bond enthalpies of mono- and bidentate formate to Cu(111). In comparison to experimental measurements on Pt(111) and Ni(111), these enthalpy values indicate that formate binds ∼15 kJ/mol more strongly to Cu(111) than to Ni(111), and ∼85 kJ/mol more strongly than to Pt(111).

At 240 K, the integral heat of the dissociative adsorption of formic acid on oxygen-predosed Cu(111) is well fit by $(99.1-46.8\theta)$ kJ/mol, which gives an integral (average) heat of 89.7 kJ/mol at 0.20 ML. The initial differential heat of adsorption is 99.1, which decreases linearly to 80.4 kJ/mol by 0.20 ML. At 120 K, the molecular adsorption of formic acid on clean Cu(111) has an initial differential heat of adsorption of 80.9 kJ/mol, which decreases to ∼70 kJ/mol by 0.50 ML. Past that coverage, the heat remains at ∼70 kJ/mol through 1.5 ML, after which it drops to a multilayer energy of 64.3 kJ/mol by 1.75 ML. Using the 120 K heat of adsorption curve measured out to multilayer coverages, we estimate the adhesion energy for liquid formic acid to Cu(111) to be 0.271 J/m^2.

These results can serve as important experimental benchmarks for DFT calculations and efforts to improve the energy accuracy of computational models. As formate is the simplest example of a carboxylate adsorbate, these results are applicable not only for systems with formate, but as well as other carboxylates and, more broadly, other oxygenates on Cu surfaces. These results further our understanding of fundamental energetic differences on catalyst surfaces, and can help explain differences in catalytic activity between late transition metal catalysts and guide the development of new catalysts and catalytic pathways.

AUTHOR INFORMATION

Corresponding Author

Charles T. Campbell − *Department of Chemical Engineering and Department of Chemistry, University of Washington, Seattle, Washington 98105-1700, United States;* orcid.org/0000-0002-5024-8210; Email: charliec@uw.edu

Authors

Griffin Ruehl − *Department of Chemical Engineering, University of Washington, Seattle, Washington 98105-1700, United States*

S. Elizabeth Harman − *Department of Chemistry, University of Washington, Seattle, Washington 98105-1700, United States*

Olivia M. Gluth − *Department of Chemical Engineering, University of Washington, Seattle, Washington 98105-1700, United States*

David H. LaVoy − *Department of Chemistry, University of Washington, Seattle, Washington 98105-1700, United States*

Complete contact information is available at: https://pubs.acs.org/10.1021/acscatal.2c02608

Author Contributions

[§]G.R. and S.E.H. share first authorship.

Notes

The authors declare no competing financial interest.

https://doi.org/10.1021/acscatal.2c02608
ACS Catal. 2022, 12, 10950−10960

■ ACKNOWLEDGMENTS

The authors acknowledge support for this work by the National Science Foundation under grant number CBET-2004757.

■ REFERENCES

(1) Ruehl, G.; Harman, S. E.; Arnadottir, L.; Campbell, C. T. Acetonitrile Adsorption and Adhesion Energies onto the Pt (111) Surface by Calorimetry. *ACS Catal.* **2022**, *12*, 156−163.
(2) Lytken, O.; Lew, W.; Campbell, C. T. Catalytic reaction energetics by single crystal adsorption calorimetry: hydrocarbons on Pt(111). *Chem. Soc. Rev.* **2008**, *37*, 2172−2179.
(3) Zhao, W.; Carey, S. J.; Mao, Z.; Campbell, C. T. Adsorbed Hydroxyl and Water on Ni(111): Heats of Formation by Calorimetry. *ACS Catal.* **2018**, *8*, 1485−1489.
(4) Carey, S. J.; Zhao, W.; Frehner, A.; Campbell, C. T.; Jackson, B. Energetics of Adsorbed Methyl and Methyl Iodide on Ni(111) by Calorimetry: Comparison to Pt(111) and Implications for Catalysis. *ACS Catal.* **2017**, *7*, 1286−1294.
(5) Karp, E. M.; Silbaugh, T. L.; Campbell, C. T. Energetics of Adsorbed CH3 and CH on Pt(111) by Calorimetry: Dissociative Adsorption of CH3I. *J. Phys. Chem. C* **2013**, *117*, 6325−6336.
(6) Silbaugh, T. L.; Karp, E. M.; Campbell, C. T. Energetics of Formic Acid Conversion to Adsorbed Formates on Pt(111) by Transient Calorimetry. *J. Am. Chem. Soc.* **2014**, *136*, 3964−3971.
(7) Ihm, H.; Ajo, H. M.; Gottfried, J. M.; Bera, P.; Campbell, C. T. Calorimetric Measurement of the Heat of Adsorption of Benzene on Pt(111). *J. Phys. Chem. B* **2004**, *108*, 14627−14633.
(8) Gottfried, J. M.; Vestergaard, E. K.; Bera, P.; Campbell, C. T. Heat of Adsorption of Naphthalene on Pt(111) Measured by Adsorption Calorimetry. *J. Phys. Chem. B* **2006**, *110*, 17539−17545.
(9) Lew, W.; Crowe, M. C.; Karp, E.; Campbell, C. T. Energy of Molecularly Adsorbed Water on Clean Pt(111) and Pt(111) with Coadsorbed Oxygen by Calorimetry. *J. Phys. Chem. C* **2011**, *115*, 9164−9170.
(10) Karp, E. M.; Campbell, C. T.; Studt, F.; Abild-Pedersen, F.; Nørskov, J. K. Energetics of Oxygen Adatoms, Hydroxyl Species and Water Dissociation on Pt(111). *J. Phys. Chem. C* **2012**, *116*, 25772−25776.
(11) Karp, E. M.; Silbaugh, T. L.; Campbell, C. T. Energetics of Adsorbed CH3 and CH on Pt(111) by Calorimetry. *J. Am. Chem. Soc.* **2013**, *135*, 5208−5211.
(12) Carey, S. J.; Zhao, W.; Harman, E.; Baumann, A.; Mao, Z.; Zhang, W.; Campbell, C. T. Energetics of Adsorbed Methanol and Methoxy on Ni(111): Comparisons to Pt(111). *ACS Catal.* **2018**, *8*, 10089−10095.
(13) Zhao, W.; Carey, S. J.; Morgan, S. E.; Campbell, C. T. Energetics of adsorbed formate and formic acid on Ni(111) by calorimetry. *J. Catal.* **2017**, *352*, 300−304.
(14) Shiozawa, Y.; Koitaya, T.; Mukai, K.; Yoshimoto, S.; Yoshinobu, J. The roles of step-site and zinc in surface chemistry of formic acid on clean and Zn-modified Cu(111) and Cu(997) surfaces studied by HR-XPS, TPD, and IRAS. *J. Chem. Phys.* **2020**, *152*, 044703.
(15) Gokhale, A. A.; Dumesic, J. A.; Mavrikakis, M. On the Mechanism of Low-Temperature Water Gas Shift Reaction on Copper. *J. Am. Chem. Soc.* **2008**, *130*, 1402−1414.
(16) Zhang, R.; Ludviksson, A.; Campbell, C. T. The chemisorption of methanol on Cu films on ZnO(0001)-O. *Catal. Lett.* **1994**, *25*, 277−292.
(17) Lin, S.; Johnson, R. S.; Smith, G. K.; Xie, D.; Guo, H. Pathways for methanol steam reforming involving adsorbed formaldehyde and hydroxyl intermediates on Cu(111): density functional theory studies. *Phys. Chem. Chem. Phys.* **2011**, *13*, 9622−9631.
(18) Chen, B. W. J.; Bhandari, S.; Mavrikakis, M. Role of Hydrogen-bonded Bimolecular Formic Acid-Formate Complexes for Formic Acid Decomposition on Copper: A Combined First-Principles and Microkinetic Modeling Study. *ACS Catal.* **2021**, *11*, 4349−4361.
(19) Li, S.; Scaranto, J.; Mavrikakis, M. On the Structure Sensitivity of Formic Acid Decomposition on Cu Catalysts. *Top. Catal.* **2016**, *59*, 1580−1588.
(20) Baber, A. E.; Mudiyanselage, K.; Senanayake, S. D.; Beatriz-Vidal, A.; Luck, K. A.; Sykes, E. C. H.; Liu, P.; Rodriguez, J. A.; Stacchiola, D. J. Assisted deprotonation of formic acid on Cu(111) and self-assembly of 1D chains. *Phys. Chem. Chem. Phys.* **2013**, *15*, 12291−12298.
(21) Putra, S. E. M.; Muttaqien, F.; Hamamoto, Y.; Inagaki, K.; Hamada, I.; Morikawa, Y. Van der Waals density functional study of formic acid adsorption and decomposition on Cu(111). *J. Chem. Phys.* **2019**, *150*, 154707.
(22) Putra, S. E. M.; Muttaqien, F.; Hamamoto, Y.; Inagaki, K.; Shiotari, A.; Yoshinobu, J.; Morikawa, Y.; Hamada, I. Theoretical study on adsorption and reaction of polymeric formic acid on the Cu (111) surface. *Phys. Rev. Mater.* **2021**, *5*, 075801.
(23) Lynch, I.; Cedervall, T.; Lundqvist, M.; Cabaleiro-Lago, C.; Linse, S.; Dawson, K. A. The nanoparticle-protein complex as a biological entity; a complex fluids and surface science challenge for the 21st century. *Adv. Colloid Interface Sci. 134-* **2007**, *135*, 167−174.
(24) Kasemo, B. Biological surface science. *Surf. Sci.* **2002**, *500*, 656−677.
(25) Barth, J. V.; Costantini, G.; Kern, K. Engineering atomic and molecular nanostructures at surfaces. *Nanoscience and Technology* **2009**, 67−75.
(26) Sarikaya, M.; Tamerler, C.; Jen, A. K.-Y.; Schulten, K.; Baneyx, F. Molecular biomimetics: nanotechnology through biology. *Nat. Mater.* **2003**, *2*, 577−585.
(27) Durand, W. J.; Peterson, A. A.; Studt, F.; Abild-Pedersen, F.; Nørskov, J. K. Structure effects on the energetics of the electrochemical reduction of CO2 by copper surfaces. *Surf. Sci.* **2011**, *605*, 1354−1359.
(28) Qiao, J.; Liu, Y.; Hong, F.; Zhang, J. A review of catalysts for the electroreduction of carbon dioxide to produce low-carbon fuels. *Chem. Soc. Rev.* **2014**, *43*, 631−675.
(29) Quan, J.; Muttaqien, F.; Kondo, T.; Kozarashi, T.; Mogi, T.; Imabayashi, T.; Hamamoto, Y.; Inagaki, K.; Hamada, I.; Morikawa, Y.; Nakamura, J. Vibration-driven reaction of CO2 on Cu surfaces via Eley-Rideal-type mechanism. *Nat. Chem.* **2019**, *11*, 722−729.
(30) Wang, Y.-F.; Li, K.; Wang, G.-C. Formic acid decomposition on Pt1/Cu(111) single platinum atom catalyst: Insights from DFT calculations and energetic span model analysis. *Appl. Surf. Sci.* **2018**, *436*, 631−638.
(31) Yoo, J. S.; Abild-Pedersen, F.; Nørskov, J. K.; Studt, F. Theoretical Analysis of Transition-Metal Catalysts for Formic Acid Decomposition. *ACS Catal.* **2014**, *4*, 1226−1233.
(32) Herron, J. A.; Scaranto, J.; Ferrin, P.; Li, S.; Mavrikakis, M. Trends in Formic Acid Decomposition on Model Transition Metal Surfaces: A Density Functional Theory study. *ACS Catal.* **2014**, *4*, 4434−4445.
(33) Pradhan, S.; Reddy, A. S.; Devi, R. N.; Chilukuri, S. Copper-based catalysts for water gas shift reaction: Influence of support on their catalytic activity. *Catal. Today* **2009**, *141*, 72−76.
(34) Appel, A. M.; Bercaw, J. E.; Bocarsly, A. B.; Dobbek, H.; DuBois, D. L.; Dupuis, M.; Ferry, J. G.; Fujita, E.; Hille, R.; Kenis, P. J. A.; Kerfeld, C. A.; Morris, R. H.; Peden, C. H. F.; Portis, A. R.; Ragsdale, S. W.; Rauchfuss, T. B.; Reek, J. N. H.; Seefeldt, L. C.; Thauer, R. K.; Waldrop, G. L. Frontiers, Opportunities, and Challenges in Biochemical and Chemical Catalysis of CO2 Fixation. *Chem. Rev.* **2013**, *113*, 6621−6658.
(35) Hori, Y.; Wakebe, H. H. I.; Tsukamoto, T.; Koga, O. Electrocatalytic Process of CO Selectivity in Electrochemical Reduction of CO2 at Metal Electrodes in Aqueous Media. *Electrochim. Acta* **1994**, *39*, 1833−1839.
(36) Nie, X.; Esopi, M. R.; Janik, M. J.; Asthagiri, A. Selectivity of CO2 Reduction on Copper Electrodes: The Role of the Kinetics of Elementary Steps. *Angew. Chemie - Int. Ed.* **2013**, *52*, 2459−2462.

https://doi.org/10.1021/acscatal.2c02608
ACS Catal. 2022, 12, 10950−10960

(37) Ajo, H. M.; Ihm, H.; Moilanen, D. E.; Campbell, C. T. Calorimeter for adsorption energies of larger molecules on single crystal surfaces. *Rev. Sci. Instrum.* **2004**, *75*, 4471−4480.
(38) Lew, W.; Lytken, O.; Farmer, J. A.; Crowe, M. C.; Campbell, C. T. Improved pyroelectric detectors for single crystal adsorption calorimetry from 100 to 350 K. *Rev. Sci. Instrum.* **2010**, *81*, 024102.
(39) King, D. A.; Wells, M. G. Molecular Beam Investigation of Adsorption Kinetics on Bulk Metal Targets: Nitrogen on Tungsten. *Surf. Sci.* **1972**, *29*, 454−482.
(40) Lew, W.; Crowe, M. C.; Karp, E.; Lytken, O.; Farmer, J. A.; Arnadottir, L.; Schoenbaum, C.; Campbell, C. T. The Energy of Adsorbed Hydroxyl on Pt(111) by Microcalorimetry. *J. Phys. Chem. C* **2011**, *115*, 11586−11594.
(41) Babar, S.; Weaver, J. H. Optical constants of Cu, Ag, and Au revisited. *Appl. Opt.* **2015**, *54*, 477−481.
(42) Weaver, J. H.; Krafka, C.; Lynch, D. W.; Koch, E. E. Optical properties of metals. *Appl. Opt.* **1981**, *20*, 1124_1−1125.
(43) Marcinkowski, M. D.; Murphy, C. J.; Liriano, M. L.; Wasio, N. A.; Lucci, F. R.; Sykes, E. C. H. Microscopic View of the Active Sites for Selective Dehydrogenation of Formic Acid on Cu(111). *ACS Catal.* **2015**, *5*, 7371−7378.
(44) Shiozawa, Y.; Koitaya, T.; Mukai, K.; Yoshimoto, S.; Yoshinobu, J. Quantitative analysis of desorption and decomposition kinetics of formic acid on Cu(111): The importance of hydrogen bonding between adsorbed species. *J. Chem. Phys.* **2015**, *143*, 234707.
(45) Sotiropoulos, A.; Milligan, P. K.; Cowie, B. C. C.; Kadodwala, M. A structural study of formate on Cu(111). *Surf. Sci.* **2000**, *444*, 52−60.
(46) Wuhn, M.; Weckesser, J.; Woll, C. Bonding and Orientational Ordering of Long-Chain Carboxylic Acids on Cu(111): Investigations Using X-ray Absorption Spectroscopy. *Langmuir* **2001**, *17*, 7605−7612.
(47) Nakano, H.; Nakamura, I.; Fujitani, T.; Nakamura, J. Structure-Dependent Kinetics for Synthesis and Decomposition of Formate Species over Cu(111) and Cu(110) Model Catalysts. *J. Phys. Chem. B* **2001**, *105*, 1355−1365.
(48) Stone, P.; Poulston, S.; Bennett, R. A.; Price, N. J.; Bowker, M. An STM, TPD and XPS investigation of formic acid adsorption on the oxygen-precovered c(6 × 2) surface of Cu(110). *Surf. Sci.* **1998**, *418*, 71−83.
(49) Nishimura, H.; Yatsu, T.; Fujitani, T.; Uchijima, T.; Nakamura, J. Synthesis and decomposition of formate on a Cu(111) surface — kinetic analysis. *J. Mol. Catal. A Chem.* **2000**, *155*, 3−11.
(50) Pöllmann, B. S.; Bayer, A.; Ammon, C.; Steinrück, H. Adsorption and Reaction of Methanol on Clean and Oxygen Precovered Cu(111). *Z. Phys. Chem.* **2004**, *218*, 957−971.
(51) Kolovos-Vellianitis, D.; Kammler, T.; Kuppers, J. Interaction of gaseous hydrogen atoms with oxygen covered Cu(100) surfaces. *Surf. Sci.* **2001**, *485*, 166−170.
(52) Bange, K.; Grider, D. E.; Madey, T. E.; Sass, J. K. The surface chemistry of H2O on clean and oxygen-covered Cu(110). *Surf. Sci.* **1984**, *137*, 38−64.
(53) Clendening, W. D.; Rodriguez, J. A.; Campbell, J. M.; Campbell, C. T. The Chemisorption and Coadsorption of Water and Oxygen on Cs-Dosed Cu(110). *Surf. Sci.* **1989**, *216*, 429−461.
(54) Habraken, F. H. P. M.; Kieffer, E. P.; Bootsma, G. A. A study of the kinetics of the interactions of O2 and N2O with a Cu(111) surface and of the reaction of CO with adsorbed oxygen using AES, LEED and ellipsometry. *Surf. Sci.* **1979**, *83*, 45−59.
(55) Karp, E. M.; Silbaugh, T. L.; Crowe, M. C.; Campbell, C. T. Energetics of Adsorbed Methanol and Methoxy on Pt(111) by Microcalorimetry. *J. Am. Chem. Soc.* **2012**, *134*, 20388−20395.
(56) Acree, Jr., W. E., Chickos, J. S. Phase Transition Enthalpy Measurements of Organic and Organometallic Compounds. In *NIST Standard Reference Database Number 69*; Linstrom, P. J., Mallard, W. G., Eds.; National Institute of Standards and Technology, 2021.
(57) Yaws, C. L. *Yaws' Handbook of Thermodynamic and Physical Properties of Chemical Compounds*; Knovel, 2003.
(58) Stephenson, R. M., Malanowski, S. *Handbook of the thermodynamics of organic compounds*; Elsevier, 1987.
(59) Carey, S. J.; Zhao, W.; Mao, Z.; Campbell, C. T. Energetics of Adsorbed Phenol on Ni(111) and Pt(111) by Calorimetry. *J. Phys. Chem. C* **2019**, *123*, 7627−7632.
(60) Carey, S. J.; Zhao, W.; Campbell, C. T. Energetics of adsorbed benzene on Ni(111) and Pt(111) by calorimetry. *Surf. Sci.* **2018**, *676*, 9−16.
(61) Campbell, C. T.; Sellers, J. R. V. Enthalpies and Entropies of Adsorption on Well-Defined Oxide Surfaces: Experimental Measurements. *Chem. Rev.* **2013**, *113*, 4106−4135.
(62) Silbaugh, T. L.; Campbell, C. T. Energies of Formation Reactions Measured for Adsorbates on Late Transition Metal Surfaces. *J. Phys. Chem. C* **2016**, *120*, 25161−25172.
(63) Dell, R. M.; Stone, F. S.; Tiley, P. F. The Adsorption of Oxygen and other Gases on Copper. *Trans. Faraday Soc.* **1953**, *49*, 195−201.
(64) Giamello, E.; Fubini, B.; Lauro, P.; Bossi, A. A Microcalorimetric Method for the Evaluation of Copper Surface Area in Cu-ZnO Catalyst. *J. Catal.* **1984**, *87*, 443−451.
(65) Wang, Y.; Yan, L.; Wang, G. Oxygen-assisted water partial dissociation on copper: a model study. *Phys. Chem. Chem. Phys.* **2015**, *17*, 8231−8238.
(66) Carey, S. J.; Zhao, W.; Campbell, C. T. Bond Energies of Adsorbed Intermediates to Metal Surfaces: Correlation with Hydrogen - Ligand and Hydrogen - Surface Bond Energies and Electronegativities. *Angew. Chemie - Int. Ed.* **2018**, *57*, 16877−16881.
(67) Luo, Y.-R. *Comprehensive Handbook of Chemical Bond Energies*; CRC Press, 2007.
(68) Wellendorff, J.; Silbaugh, T. L.; Garcia-Pintos, D.; Norskov, J. K.; Bligaard, T.; Studt, F.; Campbell, C. T. A benchmark database for adsorption bond energies to transition metal surfaces and comparison to selected DFT functionals. *Surf. Sci.* **2015**, *640*, 36−44.
(69) Grabow, L. C.; Gokhale, A. A.; Evans, S. T.; Dumesic, J. A.; Mavrikakis, M. Mechanism of the Water Gas Shift Reaction on Pt: First Principles, Experiments, and Microkinetic Modeling. *J. Phys. Chem. C* **2008**, *112*, 4608−4617.
(70) Singh, N.; Campbell, C. T. A Simple Bond-Additivity Model Explains Large Decreases in Heats of Adsorption in Solvents Versus Gas Phase: A Case Study with Phenol on Pt(111) in Water. *ACS Catal.* **2019**, *9*, 8116.
(71) Rumptz, J. R.; Campbell, C. T. Adhesion Energies of Solvent Films to Pt(111) and Ni(111) Surfaces by Adsorption Calorimetry. *ACS Catal.* **2019**, *9*, 11819−11825.
(72) Haynes, W. M.; Lide, D. R.; Bruno, T. J. *CRC Handbook of Chemistry and Physics*; CRC Press, 2016.
(73) Ohtani, T.; Kubota, J.; Wada, A.; Kondo, J. N.; Domen, K.; Hirose, C. IRAS and TPD study of adsorbed formic acid on Pt(110)-(1 × 2) surface. *Surf. Sci.* **1996**, *368*, 270−274.
(74) Chapman, D. The infrared spectra of liquid and solid formic acid. *J. Chem. Soc.* **1956**, 225−229.
(75) Redhead, P. A. Thermal Desorption of Gases. *Vacuum* **1962**, *12*, 203−211.

https://doi.org/10.1021/acscatal.2c02608
ACS Catal. 2022, 12, 10950−10960